

# Porosity dependence of thermal conductivity of ceramics and sedimentary rocks

A. S. WAGH

*Materials Laboratory, Physics Department, University of the West Indies, Mona, Kingston 7, Jamaica, West Indies, and Materials and Components Technology Division, Argonne National Laboratory, IL 60439, USA*

The connected grain model of porous ceramics, developed earlier to explain porosity dependence of the elastic modulus, is extended to study thermal transport. The porosity and grain-size dependence of the thermal conductivity is calculated in terms of a power law. The exponent of the power law is dependent on the skewness of the grain-size distribution. The formalism is compared with the experimental results for isometric spherical-pore distribution in alumina, random-pore distribution in alumina, uranium dioxide and yttria-stabilized zirconia, sedimentary rocks and bricks. Good agreements are found between the experimental results and theoretical predictions based on the microstructure of the materials and their porosity dependence of the elastic modulus.

## 1. Introduction and review of earlier work

Thermal properties of porous ceramics are of considerable practical interest, due to their potential applications in devices such as refractories [1], high-temperature gas filters [2], and heat exchangers [3]. In such devices, thermal conductivity plays a major role in heat transfer calculations. Similarly, thermal properties of rocks and concrete play an important role in several important geophysical applications, such as repositories of high-level radioactive waste [4].

Thermal conductivity of porous ceramics has been studied by a number of workers. The early work on modelling of heat flow through porous media was done by Eucken [5, 6], Russell [7], and Loeb [8]. They developed models for isometric pore shapes (spherical and cubical) and showed that the volume pore fraction increases the effective thermal conductivity of porous ceramics. Riboud [9] used a law of mixtures for thermal conductivity of a porous solid by treating the solid and air channels separately. Austin [10] and Barrett [11] gave surveys which emphasized the effects of orientation of pores, while Aivazov and Domashnev [12] developed a parametric equation for thermal conductivity as a function of porosity.

To verify some of these formalisms, Francl and Kingery [13] carried out experimental measurements on effects of isometric spherical and anisometric cylindrical pore shapes in alumina, graphite and nickel. The choice of these materials was guided by the fact that nickel, alumina and graphite have low, medium and high emissivities and hence the effect of radiation on thermal conductivity in the three materials could be compared. They showed that the thermal conductivity of such porous materials is directly proportional to the density of the material below  $\sim 500^\circ\text{C}$ , where

emissivity is low. Beyond this temperature, however, radiation from the pore surfaces affects the net thermal conductivity.

McClalland [14] measured the thermal conductivity of alumina in the porosity range 0–0.5. Mirkovich [15], and Swain *et al.* [16] measured the thermal diffusivity of porous stabilized zirconia at  $50^\circ\text{C}$ , and at elevated temperatures, respectively. Ross [17] measured the thermal conductivity of uranium dioxide. The thermal conductivity measurements in sand stones and bricks were extensive. Sugiwarra and Yoshizawa [18] studied the thermal conductivity of Iwaki and Akabira sandstones from Japan, while Woodside and Messmer [19] measured the thermal conductivity of quartz-rich sand stones. The data on silica and diaspore bricks and on limestone were given by Austin [20].

A comparison of much of the data from the works given above with theoretical formulations of Russell [7], Loeb [8] and Austin [10], and modifications of their equations, was carried out by Rhee [21]. He concludes that, overall, the experimental data agree well only with the parametric equation of Aivazov and Domashnev [12].

The lack of agreement between experiments and theoretical predictions of the models presented in the overview given above, may be because of two reasons, i.e. the models are either empirical or they assume that ceramics have geometrically regular microstructure. In practice, however, ceramics consist of random microstructures. The pores and grains have random shapes and sizes and random orientation. Thus, to incorporate this random nature of ceramic structures, there is a need for a model which describes the thermal conductivity of ceramics from first principles, in which randomness of the grain and pore sizes and their shapes forms the basis of derivation. A connected

grain model, which incorporates such random microstructure has been developed by Wagh *et al.* [22] to relate porosity with elastic modulus of ceramics. This model is extended here to thermal transport in porous structures such as sintered ceramics, bricks and sedimentary rocks. Such a generalization of the model allows one to study the porosity dependence of thermal conductivity. In addition, it allows one to relate thermal transport to mechanical properties in polycrystalline ceramics and rocks.

The model is briefly described, and is applied to thermal conductivity; the explicit dependence of the thermal conductivity on porosity in random structures is derived. The formulae derived are tested with experimental results on various ceramics, sedimentary rocks and bricks. Finally the implications of the model in practical circumstances are discussed. The details of the calculations of the contribution of radiation from the pore surfaces to the thermal conductivity are provided in the Appendix.

## 2. Connected grain model of ceramics

The connected grain model [22], which is generalized here, assumes that grains in a polycrystalline ceramic are connected to each other at random to form a three-dimensional network of materials chains. The pore structure also forms a continuous network of channels between the chains. The materials chains, as well as the pore channels, have randomly varying cross-sections along their lengths. To simulate these cross-sections, we start with a chain of uniform cross-section, divide it into imaginary cylinders of length of a typical grain size and shrink the cross-section of a randomly chosen cylinder by a fraction,  $x$ , at a time. Repeatedly, when the cylinders are chosen randomly and shrunk, one obtains a chain of randomly varying cross-sections along its length. We assume that each cylinder consists of a lattice structure, i.e. contains elastic springs representing bonds between the lattice points. These springs are responsible for the elastic and thermal properties of the material. The details may be found in [22]. Here, we highlight the results relevant to the problem of thermal transport.

The probability,  $\Phi(n)$ , of any particular cylinder shrinking  $n$  times is given by

$$\Phi(n) = [M!/(M-n)!n!](1/N)^n[(N-1)/N]^{M-n} \quad (1)$$

where  $M$  is the total number of reductions performed among  $N$  number of cylinders involved.

The average square radius  $\langle r^2 \rangle$  of the cylinders is given by the summation over  $n$ , i.e.

$$\langle r^2 \rangle = r_0^2 \sum_{n=0}^M x^{2n} \Phi(n) \quad (2)$$

where  $r_0$  is the radius of an unshrunk cylinder. The summation of the right-hand side of Equation 2 and its comparison with a similar expression for the porosity,  $p$ , of the material leads to [22]

$$\langle r^2 \rangle = r_0^2(1-p) \quad (3)$$

which implies that the average cross-section of a chain

is directly proportional to  $(1-p)$ , and hence to the bulk density of the material.

The elastic modulus of the material resulting from the lattice structure of the cylinders was studied by Wagh *et al.* [22] and the following formula for porosity dependence of the elastic modulus was derived,

$$E = E_0 (1-p)^m \quad (4)$$

where  $E_0$  is the elastic modulus of a pore-free material and  $m = \ln x^2/(x^2 - 1)$  in thermodynamic limits. The value of  $x$  and hence that of  $m$  depends on the constituents of the material and the sintering process. A smaller value of  $x$  leads to a larger value of  $m$  and vice versa. For ceramics fabricated without any sintering aid or processes which lead to accelerated grain growth such as hot pressing, etc.,  $m$  is nearly equal to 2. When rapid grain growth occurs during sintering, because of the use of sintering aids or due to pressure sintering, the grain-size distribution widens and the shrinking parameter,  $x$ , becomes small or  $m$  becomes large. These conclusions were drawn from the elasticity data on various ceramic materials [22]. We extend these concepts to thermal transport in the next section.

## 3. Thermal conductivity of consolidated porous structures

In the model described in the last section, due to thermal excitations, the springs representing lattice vibrations produce phonons or quantized vibrations. The thermal transport is a collective effect of transport of these phonons through all the chains in the solid. For such a phonon gas, the thermal conductivity may be treated by the textbook formula [23]

$$k_s = (1/3) C_v v l \quad (5)$$

where  $C_v$  is the heat capacity of the solid at constant volume,  $v$  is the magnitude of the velocity of phonons which are responsible for the heat transport, and  $l$  is the effective mean free path, i.e. the average distance travelled by the phonons between subsequent collisions with scattering centres in the material.  $C_v$  in Equation 5 is directly measurable.  $v$  is difficult to measure in a porous material due to scattering of phonons at the pore walls. However, its magnitude may be obtained by direct measurement of the elastic modulus,  $E$ , by the formula

$$E = v^2 \rho \quad (6)$$

where  $\rho$  is the density of the material. Equation 5 may be used to obtain porosity dependence of thermal conductivity. Because the heat capacity is proportional to the density of the material, one may write

$$C_v = C_{v0}(1-p) \quad (7)$$

where  $C_{v0}$  is the heat capacity of a pore-free material. The porosity dependence of  $v$  can be obtained by using Equations 4 and 6. This leads to

$$v = v_0(1-p)^{(m-1)/2} \quad (8)$$

where  $v_0$  is the phonon velocity in a pore-free material. In Equation 5,  $l$  is a parameter characteristic of

scattering mechanisms of phonons. Therefore it varies from material to material. In ceramics, if the wavelength of the lattice wave is small and comparable to the grain size of the material, phonons will be scattered by grain boundaries and this scattering mechanism will be a dominant process over other possible scattering processes. In crystals, such as KCl, this size effect was observed for crystal sizes of a few millimetres at very low temperatures ( $< 5$  K) [23]. At such low temperatures, the phonon wavelength is comparable to the crystal size. In polycrystalline ceramics, on the other hand, the average grain size itself is of the order of few micrometres and hence phonons will have comparable wavelength even at room temperature. In such cases,  $l$  will be of the order of the average grain size. Because the grain size and density of ceramics directly depend on sintering temperature and time, one may expect bigger grain sizes in ceramics, which are denser. This implies longer mean free paths in less-porous ceramics.

This dependence of the grain size on the porosity of ceramics arises from two sources. The growth of a particular grain during sintering is proportional to the surface area of contact between that grain and surrounding grains. A larger grain will have a larger area of contact with neighbouring grains. Because  $(1 - p)$  is directly proportional to the density,  $\rho$ , from Equation 5, the surface area is directly proportional to the density,  $\rho$ . In addition, the grain growth will also depend on the concentration of other grains, which are in contact with this surface area and hence will again depend also on the density of the matrix. Thus, when both of these factors are considered, grain growth during sintering will depend on  $\rho^2$ .

The rate of increase of the average volume,  $V_G$ , of a grain with respect to the density,  $\rho$ , will be given by  $\partial v_G / \partial \rho$ . Following the arguments given above, we can write

$$\frac{\partial V_G}{\partial \rho} \propto \rho^2 \quad (9a)$$

or

$$\frac{\partial V_G}{\partial \rho} = k\rho^2 \quad (9b)$$

where  $k$  is a constant. Integrating both sides of Equation 9b, we obtain

$$V_G = \frac{k}{3} \rho^3 \quad (10)$$

Because the average grain size  $G \propto V_G^{1/3}$ , we have

$$G = G_0 \frac{\rho}{\rho_0} \quad (11)$$

where  $\rho_0$  is the theoretical density of the material. The mean free path,  $l$ , is of the order of average grain size and hence from Equation 11, we have

$$l = l_0(1 - p) \quad (12)$$

Equations 7, 8 and 12 constitute basic relations, which govern the thermal conductivity in ceramics. The relevance of the individual equations in a particular

application, however, will depend on the fabrication procedure in individual systems and the temperature at which the thermal conductivity is measured. In sintered ceramics, grain growth occurs and hence all three equations will influence the thermal conductivity at room temperature. At high temperature, however, the phonon mean free path,  $l$ , is affected by other scattering mechanisms. In particular, as the temperature increases, three phonon (Umklapp) processes [23] become dominant. These processes considerably limit the thermal conductivity and  $l$  is independent of the grain size and hence the porosity.

Sedimentary rocks are formed by precipitation rather than extensive sintering, and hence the grain growth associated with sintering in ceramics will not occur in these rocks. Therefore, the mean free path will not depend on the porosity in rocks, but the heat capacity and lattice velocity will still depend on the porosity. A similar case may arise in bricks, which are not sintered to temperatures high enough to allow grain growth. These different roles of the mean free path in different materials will be elaborated with specific examples in the next section.

The discussion presented above ignores the effect of radiation of heat energy by pore surfaces. Francl and Kingery [13] showed that the radiation effects are negligible up to  $\sim 500$  °C in ceramics of low and moderate emissivity. Beyond that temperature, however, the radiation due to pore surfaces influences the effective thermal conductivity of the material considerably. To include such a radiation term, we follow the treatment by Loeb [8], who considered the transport of energy through pore surfaces as equivalent to an additional thermal conduction term. The details of the derivation are given in the Appendix, where it is shown that the additional thermal conductivity due to pores is given by

$$k_p = 8\varepsilon\sigma T^3 r_0 p \quad (13)$$

where  $\varepsilon$  is the emissivity of the pore surfaces and has a value anywhere between 0 and 1,  $\sigma$  is the Stefan-Boltzmann constant equal to  $5.735 \times 10^{-8}$  Jm<sup>-2</sup>K<sup>-4</sup>s<sup>-1</sup>, and  $T$  is the average temperature of the specimen. Because the heat transport in materials channels as well as in pore channels enhances the overall conductivity, one may write

$$K = k_s + k_p = K_0[(1 - p)^q + \delta p] \quad (14)$$

where  $K_0$  is the thermal conductivity of the pore-free material. The exponent,  $q$ , depends on the contribution of the porosity through Equations 9, 10 and 14;  $\delta$  is given from Equations 13 and 14 as

$$\delta = 8\varepsilon\sigma T^3 r_0 / K_0 \quad (15)$$

Typical numerical estimation of  $\delta$  shows that it is a small quantity compared to  $q$ , and may be considered as a correction term at temperatures up to  $\sim 1000$  K and for pore sizes of even several hundred micrometres. Most of the experiments satisfy these conditions. This allows one to write Equation 14 approximately as

$$K = K_0(1 - p)^{q-\delta} \quad (16)$$

Equation 16 gives the porosity dependence of the effective thermal conductivity of ceramics.

#### 4. Comparison with experimental results

The model developed in the previous sections is applied to different porous structures in this section. We consider data on ceramics with isometric pore distribution, ceramics which are well sintered and have random pore size and distribution, sedimentary rocks, and bricks fired below sintering temperatures. We compare these data with Equation 16. In each case, the porosity dependence of the heat capacity, the velocity of lattice vibrations and the mean free path are examined and the porosity dependence of the thermal conductivity is derived. The exponents are calculated from the elasticity exponents from Wagh *et al.* [22]. These exponents are also obtained from the best fits with experimental data. Both sets of values of the exponents are compiled in Table I for the sake of ready comparison.

Francl and Kingery [13] extensively studied alumina ceramics with isometric pore distribution. Pores of spherical shape and equal size were formed using pore formers during sintering in their samples. Thus, the pore-size distribution was uniform. Because of this, one expects the shrinkage parameter,  $x$ , to be equal to 1 in the connected grain model described in Section 2. Using the definition of  $m$  in Equation 6 it is simple to show that

$$m = \lim_{x \rightarrow 1} [\ln x^2 / (x^2 - 1)] = 1. \quad (17)$$

For this value of  $m$ , from Equation 8, one can show that the velocity,  $v$ , of the lattice wave does not depend

on the porosity. Further, the variation in the porosity was attained by using varying pore former content in different samples, but by sintering them at the same temperature and for the same length of time. This should result in the same average grain size in all samples even though the porosity may be different. Because the mean free path is of the order of the grain size, this will result in the same mean free path in all the samples. Therefore, there should be no dependence of the mean free path on the porosity. This means, the only contribution to the porosity dependence of thermal conductivity given by Equation 5, arises from the dependence of the heat capacity on the porosity given by Equation 7. Therefore, Equation 16 may be cast in the following form

$$K = K_0(1 - p)[1 - \delta(T)] \quad (18)$$

If the temperature of the material is not very high (typically  $\sim 500^\circ\text{C}$ ), from Equation 15,  $\delta \ll 1$  for materials with moderate conductivity and pore size of  $r_0 \approx 1$  mm. In such cases,  $\delta$  may be ignored and Equation 18 may be written approximately in the form

$$K = K_0(1 - p) \quad (19)$$

Equation 19 was empirically proposed and experimentally verified for alumina for temperatures  $< 500^\circ\text{C}$  by Francl and Kingery [13]. At higher temperatures, however, radiation term affects the porosity dependence and  $\delta(T)$  cannot be ignored. Therefore, Equation 18, instead of Equation 19 had to be used at higher temperatures.

Equation 18 was fitted with experimental data of Francl and Kingery [13] and the fittings are shown in

TABLE I Exponents  $q$  obtained by fitting the equation  $K = K_0(1 - p)^q$  with various experimental results by linear regression analysis

| Material  | $q$ (exp.) | $q$ (theor) | $K_0$ (Kcal h <sup>-1</sup><br>°C <sup>-1</sup> m <sup>-1</sup> ) | Reference | Comments                                 |
|---|------------|-------------|---|-----------|--|
| Al <sub>2</sub> O <sub>3</sub> , spherical isometric, pores |            |             |   |           |  |
| Room temp.,   | 1          | 1           | —   | [12]      | Independent of pore size                 |
| 400°C   | 1.04       | 1           | —   | [12]      | Independent of pore size                 |
| 800°C, pore size 0.82 mm                                    | 0.92       | 0.9         | —   | [12]      | Contribution of radiation term           |
| 800°C, pore size 1.46 mm                                    | 0.78       | 0.8         | —   | [12]      | Contribution of radiation term           |
| Al <sub>2</sub> O <sub>3</sub> , random pore distr.         | 2.58       | 2.57        | —   | [13, 20]  | $q$ agrees with elasticity exponent      |
| UO <sub>2</sub>   | 1.48       | 1.63        | 2.99  | [16, 20]  | Mean free path constant                  |
| Y <sub>2</sub> O <sub>3</sub> -stab. ZrO <sub>2</sub>       |            |             |   |           |  |
| 25°C  | 3.1        | —           | 3.4   | [15]      | Yttria is sintering aid                  |
| 300°C   | 2.1        | —           | 2.4   | [15]      |  |
| 600°C   | 2.0        | —           | 2.5   | [15]      |  |
| Sedimentary rocks   |            |             |   |           |  |
| Akabira, Iwaki sandstones                                   | 1.4        | 1.5         | 1.38  | [17, 20]  | No grain growth                          |
| Limestone   | 1.6        | 1.5         | 1.02  | [20]      | No grain growth                          |
| Quartz-rich sandstone                                       | 3.0        | —           | 1.1   | [18, 20]  | Quartz may widen grain-size distribution |
| Bricks  |            |             |   |           |  |
| Fire brick  | 1.8        | 1.5         | 1.18  | [19, 20]  | No grain growth                          |
| Diaspore brick  | 1.8        | 1.5         | 3.18  | [19, 20]  | No grain growth                          |
| Silica brick  | 1.4        | 1.5         | 1.58  | [19, 20]  | No grain growth                          |

Fig. 1. Using these fittings, the values of  $d$  were obtained for pore sizes 0.82 and 1.46 mm. At room temperature and 400 °C, the straight-line graphs of  $\ln(1-p)$  and  $\ln(K/K_0)$  almost coincide with each other giving a slope of  $\sim 1$ . This implies that Equation 19 is valid and there is no measurable effect of radiation. At 800 °C, however, the slopes differ for the two pore sizes. Using these values of the slopes and Equation 18, the values of  $\delta(T)$  were determined. To compare them with the theoretical prediction, the values of  $\delta$  were also calculated using Equation 15. The values of  $K_0$  and  $\epsilon$  for alumina were assumed to be  $\sim 2.988 \text{ J m}^{-1} \text{ K}^{-1}$  and  $\sim 1$ , respectively. The theoretically determined values, as well as those obtained from the best fit in Fig. 1, are shown in Table II. The close agreement between these values confirms the applicability of the model to alumina with isometric pore distribution.

When ceramics are sintered at different temperatures and the porosity is reduced by grain growth, the contribution to the porosity dependence of the thermal conductivity arises from all three factors, i.e. heat capacity, lattice velocity and mean free path, as given by Equations 7, 8 and 12. Thus, the expression for the thermal conductivity, in the absence of a radiation term may be written from Equation 16 by

$$K = K_0(1-p)^q \quad (20)$$

where  $q = (m+3)/2$ .

The data by McClelland [14] for alumina is fitted with Equation 20 in Fig. 2 with  $q = 2.58$  for the best fit. The value of  $m$  for alumina was shown earlier [22] to be equal to 2.14 from the elasticity measurements. For this value of  $m$ , one expects  $q$  to be 2.57 from

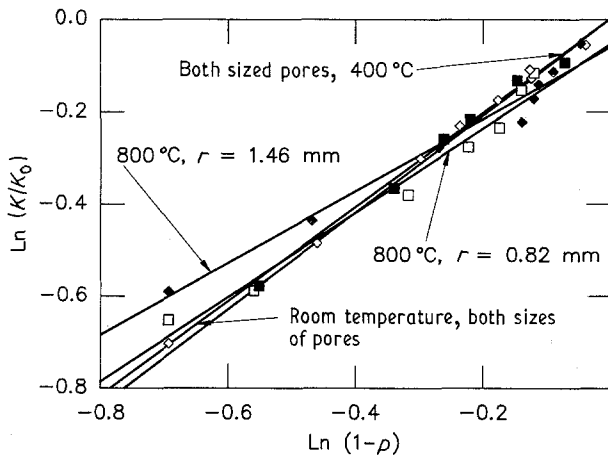


Figure 1 Porosity dependence of thermal conductivity of alumina at different temperatures with isometric spherical pore distribution fitted to the equation  $K = K_0(1-p)^{1-\delta}$ .

TABLE II Theoretically and experimentally determined values of the radiation term (Equation 15) for isometric pore distribution at 800 °C in alumina

| Pore size (mm) | $\delta$ (theoretical) | $\delta$ (experimental) |
|----------------|------------------------|-------------------------|
| 0.82           | $\sim 0.1$             | 0.08                    |
| 1.46           | $\sim 0.2$             | 0.22                    |

Equation 20 for alumina. This is very close to the value of 2.58 obtained from the best fit, confirming the consistency of the connected grain model in applications to mechanical as well as thermal properties.

A similar comparison of Equation 20 with experimental results on  $\text{UO}_2$  by Ross [17] is shown in the same figure. The value of  $q$  obtained by the best fit is 1.48. It has been shown in earlier work [22] that the value for  $m$  from the elasticity data is 2.27. A value very close to this is obtained by assuming that the mean free path is constant and independent of grain size. The mean free path may be constant because processes such as the Umklapp process limited the mean free path, or may be due to the fact that  $\text{UO}_2$  was not sintered enough to allow grain growth. In any case, when the mean free path does not depend on the porosity, Equation 16 reduces to

$$K = K_0(1-p)^{(m+1)/2} \quad (22)$$

From the elasticity data the calculated exponent was  $(m+1)/2 = 1.63$ , which is close to that obtained from the best fit.

The thermal conductivity results of yttria-stabilized zirconia are fitted with the theoretical prediction of the model in Fig. 3. The data agree quite well with Equation 20 at all three temperatures. At 25 °C, the

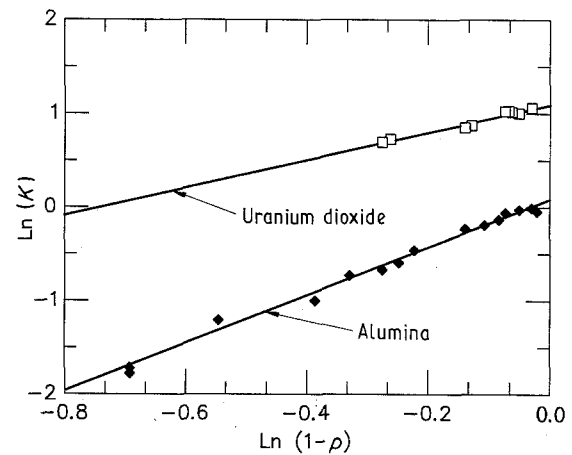


Figure 2 Variation of thermal conductivity with porosity of alumina and uranium dioxide.

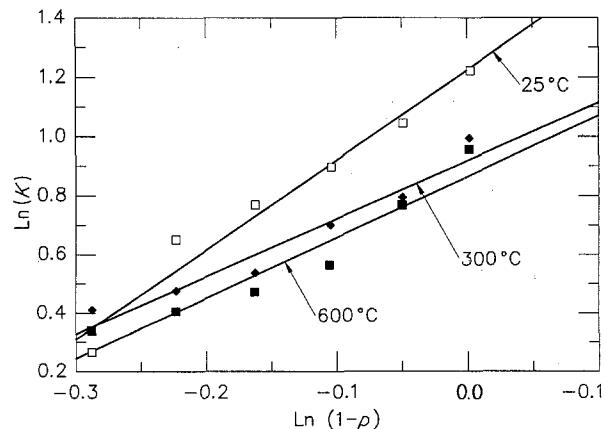


Figure 3 Porosity dependence of thermal conductivity of yttria-stabilized  $\text{ZrO}_2$ .

value of  $q$  was found to be 3.1. Using the relation between  $q$  and  $m$  given by Equation 20, we obtain  $m = 3.2$ , which is higher than the value obtained for alumina. Noting the fact that yttria, which is a glassy-phase material, is a sintering agent added for the purpose of stabilization, might have also helped in rapid densification in the material. A similar effect was reported [22] with the elasticity measurements of silicon nitride sintered with yttria as a sintering agent and the present conclusion is consistent with it. At 300 and 600 °C, the values of  $q$  are 2.1 and 2.0. At these temperatures, the phonon mean free path is limited by other scattering mechanisms, such as Umklapp process [23], and hence is independent of the grain size. Thus one expects that the porosity dependence of the thermal conductivity will arise from its dependence on the heat capacity and lattice velocity only. As a result,  $m$  may be evaluated by the expression  $q = (m + 1)/2$ . This yields a value of 3.2 for  $m$  at 300 °C, which is the same value at 25 °C. The slight decrease in the value of  $q$  at 600 °C is likely to be due to the radiation by the pore surfaces. If this is true,  $\delta = 0.1$ , which is of the same order of magnitude as that was found in alumina in the preceding discussion.

Consolidated rocks are formed by precipitation, rather than sintering. Thus, grains do not grow during their formation. Therefore the relevant equation to be used is Equation 22. The agreement of this equation with the data is shown in Fig. 4, which shows the fitting of thermal conductivity data on different sedimentary rocks with Equation 22. In the case of Akabira, Iwaki sandstones and limestone, the value of  $(m + 1)/2$  is nearly 1.5. Considering the fact that there is no contribution due to the mean free path in these materials, this value of  $q$  yields  $m = 2$ . This is quite consistent with earlier conclusions [22], that in the absence of any sintering aids, random porosity should result in a value of  $m$  of nearly 2. Wong *et al.* [24] observe a similar exponent for the porosity dependence of permeability of porous rocks. Considering the fact that the skewness of the materials as well as pore channels is the same for a given ceramic [22], this agreement of the exponents obtained in materials-related transport of thermal conductivity and pore-

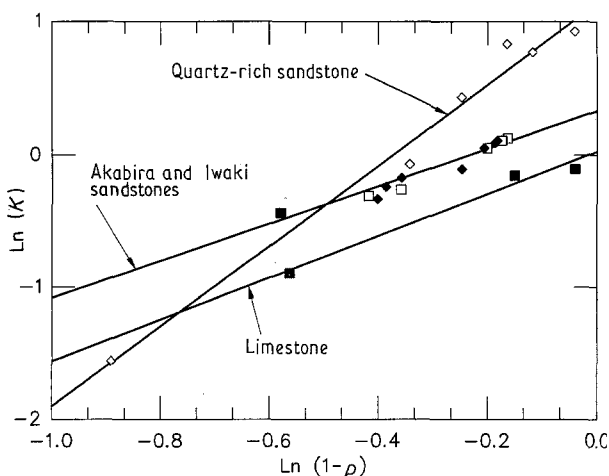


Figure 4 Dependence of the thermal conductivity on porosity of sedimentary rocks.

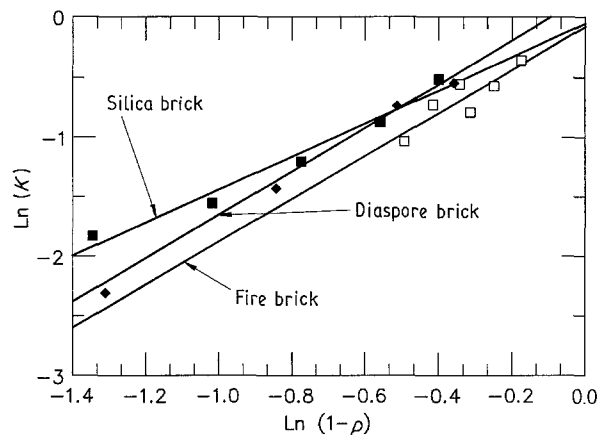


Figure 5 Porosity dependence of thermal conductivity of bricks.

related transport of fluid permeability, is not surprising. In the quartz-rich sandstones, however, the value of  $(m + 1)/2$  is 3. The presence of quartz is likely to widen the grain-size distribution and hence the skewness of the cross-section of the material chains. This should result in a smaller value of  $x$  and hence a larger value of  $m$ . This inference could not be verified because no data on microstructure were available on quartz-rich sandstone.

Finally, we present the data on bricks in Fig. 5. Bricks are fired until the water of crystallization escapes the material. Thus, they are not sintered to high temperatures to attain any grain growth. Thus, one would expect a value of  $m = 2$  and  $q = (m + 1)/2 = 1.5$ . The data on bricks confirm this. For silica brick, we obtained a value of 1.5, and for diaspore and fire bricks, a value of 1.8. This means that in these materials the mean free path does not depend on the porosity and thermal conductivity is governed by the porosity dependence of the heat capacity and the lattice wave velocity.

## 5. Implications of the connected grain model

The connected grain model presented here relates the thermal conductivity to the microstructure, such as the average grain size and the grain-size distribution. It provides an explicit dependence of the thermal conductivity on the porosity in terms of  $q$  of a power law given by Equation 16. In the process, it provides some deeper insights into the required processes to fabricate ceramics of desired thermal conductivity. The exponent, which is a measure of the skewness of the pore-size distribution, governs the conductivity for a given porosity. Thus, the thermal conductivity may be manipulated by controlling the average pore size and pore-size distribution.

The connected grain model also makes a direct connection between the mechanical and fracture properties of the material. Such a connection between the thermal conductivity and the modulus of elasticity is already exhibited in the last section. Similar relations between the fracture properties and the modulus of elasticity will be discussed in a future publication [25], by which, connections can be made between the thermal conductivity and the fracture behaviour of the

materials. Such connections are very useful in the development of ceramic materials, where often compromises are needed between the desired thermal properties and corresponding mechanical, as well as fracture properties of these materials. The connected grain model provides such a connection.

### Appendix. Calculation of the radiation term in Equation 18

Consider the transfer of heat across the facing walls of a pore channel of average diameter  $2\langle r \rangle$ . The walls will be at a temperature difference of  $\delta T$ , due to the overall constant temperature gradient existing in the system and is given in this case by  $\delta T/2\langle r \rangle$ . The heat transfer will take place due to radiation from the wall of higher temperature to the wall of lower temperature. The rate of heat transfer is given by

$$\delta Q = \varepsilon\sigma(T_1^4 - T_2^4) = 4\varepsilon\sigma T^3 \delta T \quad (\text{A1})$$

where  $\varepsilon$  and  $\sigma$  are the emissivity of the pore surface and the Stefan–Boltzmann constant,  $T_1$ ,  $T_2$  and  $T$  are the higher, lower and average temperatures, respectively. One can now approximately write from Equation A1

$$\delta Q = 4\varepsilon\sigma T^3 2\langle r \rangle \delta T \quad (\text{A2})$$

where  $dT/dx$  is the temperature gradient in the system. This leads to an equivalent thermal conductivity of the pore as

$$k_p = 8\varepsilon\sigma T^3 \langle r \rangle \quad (\text{A3})$$

It has been argued in Section 3 that the average grain size is proportional to  $(1-p)$  in a materials chain. With the same argument, one can also show that the average pore radius  $\langle r \rangle$  will be directly proportional to  $p$  in a pore channel. Thus, one can write

$$\langle r \rangle = r_0 p \quad (\text{A4})$$

where  $r_0$  is the maximum pore size in the material. This leads to

$$\begin{aligned} k_p &= 8\varepsilon\sigma T^3 r_0 p \\ &= \delta K_0 p \end{aligned} \quad (\text{A5})$$

where  $\delta = 8\varepsilon\sigma T^3 r_0/K_0$ .

### References

1. L. P. KREITZ, R. E. FISHER and J. G. BEETZ, *Ceram. Bull.* **69** (1990) 1690.
2. M. A. ALVIN, T. E. LIPPERT and J. E. LANE, *ibid.* **70** (1991) 1491.
3. J. MECHOLSKY Jr, *ibid.* **68** (1989) 369.
4. G. C. WICKS and W. A. ROSS (eds), "Nuclear Waste Management, Advances in Ceramics", Vol. 8, (American Ceramic Society, Westerville, OH, (1984) p. 746.
5. A. EUCKEN, *Ceram. Abstr.* **11** (1932) 576.
6. *Idem*, *ibid.* **12** (1933) 231.
7. H. W. RUSSELL, *J. Amer. Ceram. Soc.* **18** (1935) 1.
8. ARTHUR L. LOEB, *ibid.* **37** (1954) 96.
9. M. RIBAUD, *Chaleur Ind.* **18** (1937) 36.
10. J. B. AUSTIN, *Ceram. Abstr.* **20** (1941) 45.
11. L. R. BARRETT, *Trans. Brit. Ceram. Soc.* **48** (1949) 235.
12. M. I. AIVAZOV and I. A. DOMASHNEV, *Poroshkovaya Met.* **8** (1968) 51.
13. J. FRANCL and W. D. KINGERY, *J. Amer. Ceram. Soc.* **37** (1954) 99.
14. J. D. McCLELLAND, "Materials and Structures", Physical Measurements Program, US Air Force Report No. TDR - 930 TR-1 (1962) p. 2240.
15. VLADIMIR V. MIRKOVICH, *High Temp. High Press.* **8** (1976) 231.
16. M. V. SWAIN, L. F. JOHNSON, R. SYED and D. P. H. HASSELMAN, *J. Mater. Sci. Lett.* **5** (1986) 799.
17. A. M. ROSS, "The Dependence of the Thermal Conductivity of Uranium Dioxide on Density, Microstructure, Stoichiometry and Thermal-Neutron Irradiation", Atomic Energy of Canada Ltd, CRFD - 817 (1960).
18. A. SUGIWARA and Y. YOSHIZAWA, *J. Appl. Phys.* **33** (1962) 3135.
19. W. WOODSIDE and J. H. MESSMER, *ibid.* **32** (1961) 1699.
20. J. B. AUSTIN, in "Symposium on Thermal Insulating Materials" (American Society for Testing and Materials, Philadelphia, PA, (1939) p. 3.
21. S. K. RHEE, *Mater. Sci. Engng* **20** (1975) 89.
22. A. S. WAGH, J. P. SINGH and R. B. POEPEL, *J. Mater. Sci.* **26** (1991) 3862.
23. C. KITTEL, "Introduction to Solid State Physics" (John Wiley & Sons Inc., 1970)
24. P. WONG, J. KOPLIK and J. P. TOMANIC, *Phys. Rev B* **30** (1984) 6606.
25. ARUN S. WAGH, J. P. SINGH and R. B. POEPEL, *J. Mater. Sci.* (in print).

Received 8 November 1991  
and accepted 25 June 1992